Glycobiology vol. 17 no. 6 pp. 1C–11C, 2007
doi:10.1093/glycob/cwm030
Advance Access publication on March 16, 2007

Characterization of glycoinositolphosphoryl ceramide structure mutant strains of *Cryptococcus neoformans*

Ana LS Gutierrez[2], Layla Farage[2], Manuel N Melo[2], Ronaldo S Mohana-Borges[2], Yann Guerardel[3], Bernadete Coddeville[3], Jean-Michel Wieruszeski[3], Lucia Mendonça-Previato[1,2], and Jose O Previato[2]

[2]Instituto de Biofísica Carlos Chagas Filho, Universidade Federal do Rio de Janeiro, Cidade Universitária, 21944979, Rio de Janeiro, Brasil; and [3]Unité de Glycobiologie, Structurale et Fonctionnelle, Université des Sciences et Technologies de Lille, 59655, Villeneuve D'Ascq, France

Received on February 16, 2007; revised on March 7, 2007; accepted on March 11, 2007

In fungi, glycoinositolphosphoryl ceramide (GIPC) biosynthetic pathway produces essential molecules for growth, viability, and virulence. In previous studies, we demonstrated that the opportunistic fungus *Cryptococcus neoformans* synthesizes a complex family of xylose-(Xyl) branched GIPCs, all of which have not been previously reported in fungi. As an effort to understand the biosynthesis of these sphingolipids, we have now characterized the structures of GIPCs from *C. neoformans* wild-type (KN99α) and mutant strains that lack UDP-Xyl, by disruption of either UDP-glucose dehydrogenase (NE321) or UDP-glucuronic acid decarboxylase (NE178). The structures of GIPCs were determined by a combination of nuclear magnetic resonance (NMR) spectroscopy, tandem mass spectrometry (MS), and gas chromatography-MS. The main and largest GIPC from wild-type strain was identified as an α-Man*p*(1→6)α-Man*p*(1→3)α-Man*p*[β-Xyl*p*(1→2)]α-Man*p*(1→4)β-Gal*p*(1→6)α-Man*p*(1→2)Ins-1-P-Ceramide, whereas the most abundant GIPC from both mutant strains was found to be an α-Man*p*(1→3)α-Man*p*(1→4)β-Gal*p*(1→6)α-Man*p*(1→2)Ins-1-P-Ceramide. The ceramide moieties of *C. neoformans* wild-type and mutant strains were composed of a C_{18} phytosphingosine, which was *N*-acylated with 2-hydroxy tetra-, or hexacosanoic acid, and 2,3-dihydroxy-tetracosanoic acid. Our structural analysis results indicate that the *C. neoformans* mutant strains are unable to complete the assembly of the GIPC-oligosaccharide moiety due the absence of Xyl side chain.

Key words: Cryptococcus neoformans/*Cryptococcus* mutants/glycoinositolphosphoryl ceramide/mass spectrometry/NMR spectroscopy/UDP-Xyl

Introduction

Opportunistic fungi present an increasing threat in immunosuppressed individuals due to acquired immune deficiency syndrome (AIDS), lymphoproliferative disorders, or under treatment after organ transplantation (Mitchell and Perfect 1995). Many of the drugs available to treat fungal diseases are difficult to administer, are not effective or toxic, and some of them are becoming less useful due to the selection of more resistant strains. These facts show that more effective drugs and the discovery of new antifungal therapeutic targets are of the priority importance.

Glycoinositolphosphoryl ceramide (GIPC) is a class of glycolipid widely distributed among fungus and appears to have no exact counterpart in mammalian cells. In *Saccharomyces cerevisiae*, mutants that do not synthesize inositolphosphoryl ceramide (IPC) are not viable (Nagiec et al. 1997; Dickson and Lester 2002), and pathogenic fungi are killed when treated with compounds such as khafrefungin (Mandala et al. 1997), rustmicin (Mandala et al. 1998), and aureobasidin A (Takesako et al. 1993; Zhong et al. 2000) inhibitors of IPC synthase, an enzyme that catalyzes the transfer of phosphoinositol from phosphatidylinositol to phytoceramide to give IPC. Therefore, the enzymes catalyzing the synthesis of phosphorylinositol-containing sphingolipids have been considered potential targets for antifungal drugs.

IPC and its glycosylated derivatives, mannose inositol phosphoryl ceramide (MIPC), and mannose diinositol diphosphoryl ceramide [$M(IP)_2C$] were first characterized in *S. cerevisiae* (Smith and Lester 1974). In pathogenic and opportunistic fungi, similar compounds have been identified, however, more elaborated GIPCs have been characterized in *Aspergillus* (Bennion et al. 2003), *Histoplasma capsulatum* (Barr and Lester 1984; Barr et al. 1984), *Candida albicans* (Mille et al. 2004), *Paracoccidioides brasiliensis* (Levery et al. 1998), *Sporothrix schenckii* (Penha et al. 2000, 2001), and *Cryptococcus neoformans* (Heise et al. 2002). Despite the GIPC structures of these fungi have been characterized, few examples have shown the functional roles of their glycan moiety (Thevissen et al. 2000; Mille et al. 2004; Zink et al. 2005).

Analysis of GIPCs in *C. neoformans* has revealed the expression of a variety of Xyl-branched glycan structures, all of which have not been previously reported in fungi (Heise *et al.* 2002). *C. neoformans*, the causative agent of cryptococcosis (Mitchell and Perfect 1995), is an encapsulate fungus. The major specific virulence determinants are the capsule polysaccharides: glucuronoxylomannan (GXM) and galactoxylomannan (GalXM) (Mitchell and Perfect 1995). *C. neoformans*, presents four serotypes, is an invasive opportunistic pathogen in AIDS patients that cause most of the fungal meningitis worldwide (Mitchell and Perfect 1995).

[1]To whom correspondence should be addressed; Tel: +55 21 2562 6646; Fax: +55 21 2280 8193; E-mail: luciamp@biof.ufrj.br

To better understand the expression and distribution of GIPCs on cryptococcal plasma membrane, we determined the structure of GIPCs from *C. neoformans* wild-type (KN99α strain) (Nielsen et al. 2003) and mutant strains which lack UDP-Xyl, by disruption of either UDP-Glucose dehydrogenase (NE321 strain) (Moyrand and Janbon 2004) or UDP-glucuronic acid decarboxylase (NE178 strain) (Moyrand et al. 2002) genes. We show here structural variation between mutants and wild-type cells, and that Xyl side chain is essential for *C. neoformans* to elongate the GIPC glycan chain.

Results

Isolation, carbohydrate, and lipid composition of GIPC from C. neoformans

GIPCs isolated by aqueous phenol extraction and solubilized in chloroform/methanol/water were purified by hydrophobic chromatography on octyl-sepharose column.

On high-performance thin layer chromatography (HPTLC), the purified GIPCs of each *C. neoformans* strains migrated as a double band. The relative migration (R_f) values of GIPC from NE178 and NE321 mutants were identical and higher than that found for GIPC of KN99α wild-type strain (Figure 1). Carbohydrate composition determined by gas chromatography (GC) and GC-mass spectrometry (MS) showed that the wild-type strain contained mannose (Man), galactose (Gal), Xyl, and inositol (Ins) in a molar ratio of 4:1:1:1, respectively, whereas, the mutant strains contained Man, Gal, and Ins a molar ratio of 3:1:1. The ceramide analysis showed the presence of C_{18} phytosphingosine *N*-acylated with 2-hydroxy tetra-, hexacosanoic, or 2,3-dihydroxy tetracosanoic in GIPCs from both wild-type and mutant strains (data not shown).

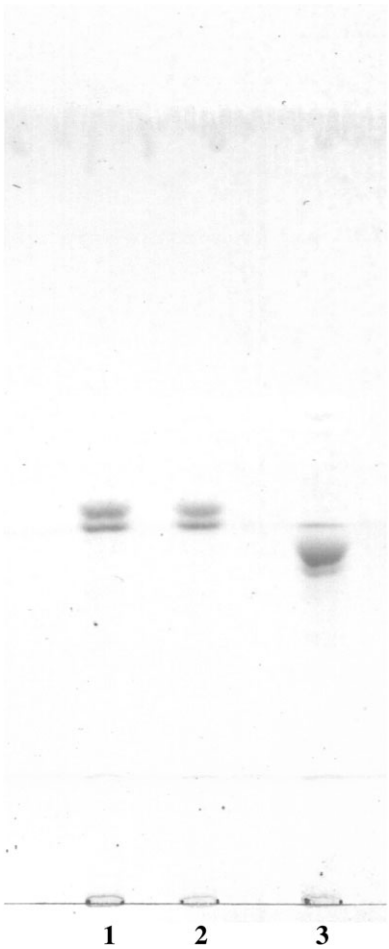

Fig. 1. HPTLC analysis of GIPCs from *C. neoformans* wild-type (KN99α) and mutant strains (NE178) and (NE 321). (**1**) NE321; (**2**) NE178; (**3**) KN99.

In agreement with the chemical composition, the negative-mode matrix-assisted laser desorption/ionization time-of-flight (MALDI-TOF) spectrum of the GIPCs from *Cryptococcus* strains shows a set of deprotonated molecules from which the carbohydrate chain size, ceramide type, and relative homogeneity can be deduced (Figure 2). In the spectrum of GIPC from the wild-type strain (Figure 2A), three deprotonated molecules were observed at m/z 1868.4, 1884.3, and 1896.4. The increment of 16 mu between m/z 1868.4 and 1884.3, and of 28 mu between 1868.4 and 1896.4 does not fit any known monosaccharide, but is consistent with the presence of three phytoceramide species composed of *t*18:0 phytosphingosine *N*-acylated with hydroxi-tetra, dihydroxi-tetra, and hydroxi-hexacosanoic acids, respectively, linked to a PI-oligosaccharide containing Pen_1Hex_5InsP.

The spectrum of NE321 mutant GIPC (Figure 2B) was apparently more complex, with two triplet groups of deprotonated molecules at m/z 1574.0, 2589.0, 1660.2, and 1736.2, 1752.2, and 1764.2. The m/z difference of 162 between the two triplet groups suggest the presence of two series of glycoinositolphosphoryl phytoceramides, differing in the composition of their fatty acid, and containing four or five Hex residues. Thus, the MALDI-TOF analysis showed that the signals in the main triplet of the NE321 mutant GIPC at m/z 1574.0, 1159.0, and 1660.2 (Figure 2B) differ from the corresponding peaks in wild-type GIPC at m/z 1868.4, 1884.3, and 1896.4 (Figure 2A) by the mass of one Pent and one Hex residues (294). The spectrum of GIPC from NE178 mutant (Figure 2C) showed one set of deprotonated molecule at m/z 1574.0, 1590.0, and 1602.1, consistent with a composition of Hex_4InsP linked to phytoceramide species identical to those described for NE321 mutant and wild-type strains.

Characterization of PI-oligosaccharides by ESI-MS

To determine the sequence of monosaccharide residues, the GIPCs were submitted to alkaline hydrolysis and the released PI-oligosaccharide was permethylated and analyzed by electrospray ionization-MS (ESI-MS) and ESI-MS/MS.

In agreement with MALDI-MS of intact GIPCs (Figure 2), PI-oligosaccharides from the three *Cryptococcus* strains exhibit different profiles in ESI-MS. The ESI analysis of permethylated PI-oligosaccharides from wild-type (Figure 3A) showed a major $[M + Na]^+$ pseudomolecular ion at m/z 1561 attributed to a Pen_1Hex_5InsP. Along this major signal, minor ions at m/z 1357, 1467, and 1263 were attributed to Pen_1Hex_4InsP, Pen_1Hex_5Ins, and Pen_1Hex_4Ins, respectively. The last two seem to be the result of the loss of phosphate group from the two corresponding phosphorylated oligosaccharides during the alkaline hydrolysis, as proved further by MS/MS sequencing (data not shown). The ESI analysis of NE321 mutant (Figure 3B) shows a major $[M + Na]^+$ pseudomolecular ion at m/z 1197 attributed to Hex_4InsP, as well as

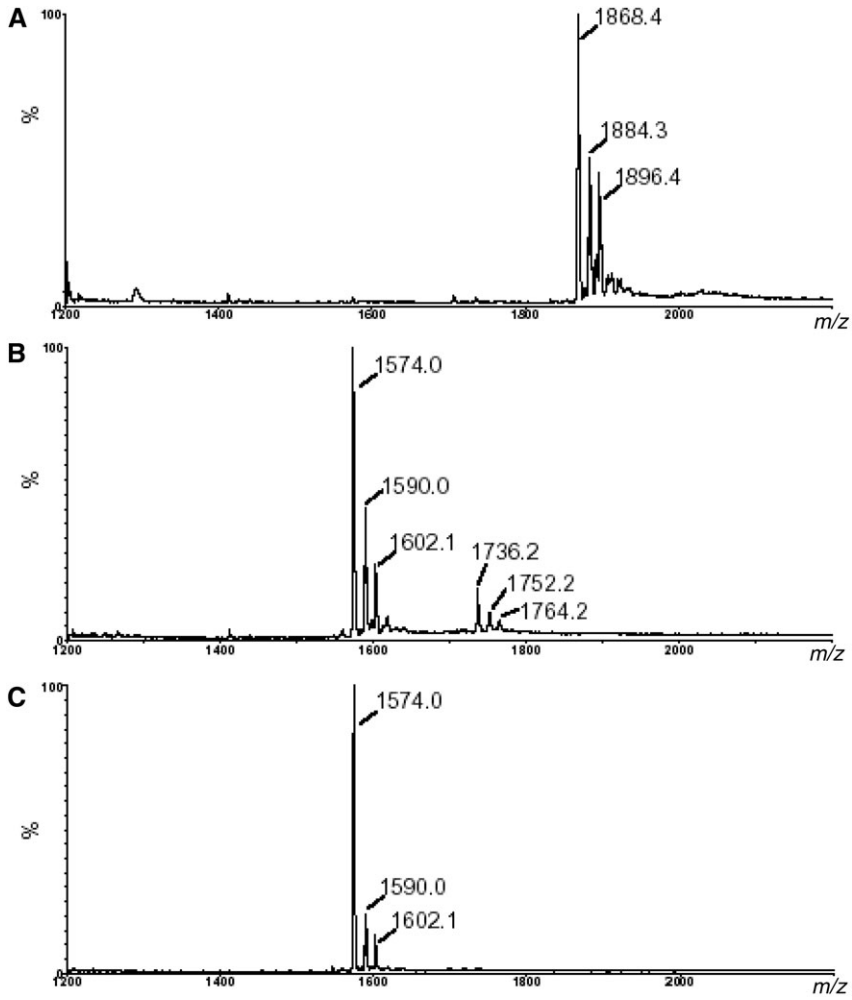

Fig. 2. Negative mode MALDI-TOF MS spectra of GIPCs from *C. neoformans* strains. (**A**) KN99α; (**B**) NE321; and (**C**) NE178.

a minor ion at m/z 1401 attributed to Hex_5InsP. As for PI-oligosaccharides from wild-type GIPCs, both phosphorylated oligosaccharides from NE321 mutant GIPCs are accompanied by their dephosphorylated counterparts at m/z 1103 and 1307, respectively. The PI-oligosaccharide ESI-MS of NE178 mutant (Figure 3C) only shows the presence of Hex_4InsP and Hex_4Ins at m/z 1197 and 1103, respectively. In conclusion, the nature of alkali released PI-oligosaccharide is consistent with the analysis of intact GIPC. GIPCs isolated from *Cryptococcus* mutant strains, NE321 and NE178, clearly differ from those purified from wild-type by the absence of pentose (Pen) unit in their oligosaccharide chains, and by fewer hexose (Hex) residues on average (four instead of five). Furthermore, PI-oligosaccharide from NE321 mutant slightly differs from NE178 mutant due to the presence of a minor amount of PI-pentasaccharide (Hex_5InsP) together with the major component PI-tetrasaccharide (Hex_4InsP).

The structure of released PI-oligosaccharides was further assessed by fragmentation analysis of their permethylated derivatives by ESI-MS/MS. Fragmentation pattern in positive mode of daughter ions at m/z 1561 from *Cryptococcus* wild-type strain (Figure 4) is characterized by the easy loss of di-methylated phosphoryl group as a B-type fragment ion at m/z 1435. Then recurrent cleavages of Hex linkages were observed as secondary B/Y and C/Y fragment ions. Their counterparts from nonreducing end were also observed as C-type ions. Observation of intense B/Y type fragment ions at m/z 1217, 1013, 649, 445, and 241 is consistent with a major Hex-Hex-[Pen]-Hex-Hex-Hex-InsP structure, where the branching point is located at the third Hex unit distal from the Ins residue. Positioning of the Pen residue is confirmed by the presence of $^{3,5}A$ ring cleavages at m/z 1101 and 897. A very similar fragmentation pattern was observed for the permethylated derivative of Pen_1Hex_4InsP from wild-type at m/z 1357 (data not shown) than for the permethylated derivative of Pen_1Hex_5InsP (Figure 4). Both PI-oligosaccharides only differ by the presence of a terminal nonreducing Hex unit.

Similar fragmentation patterns were also obtained from sodium cationized permethylated PI-oligosaccharides from the NE321 (Figure 5A) and NE178 (Figure 5B) *Cryptococcus* mutants. As observed, fragmentation of pseudomolecular ion at m/z 1197 from both mutant strains showed similar patterns indicative of a linear PI-oligosaccharide Hex-Hex-Hex-Hex-InsP. They are characterized by recurrent releases of Hex units from nonreducing end as Y-type ions as well as B/Y

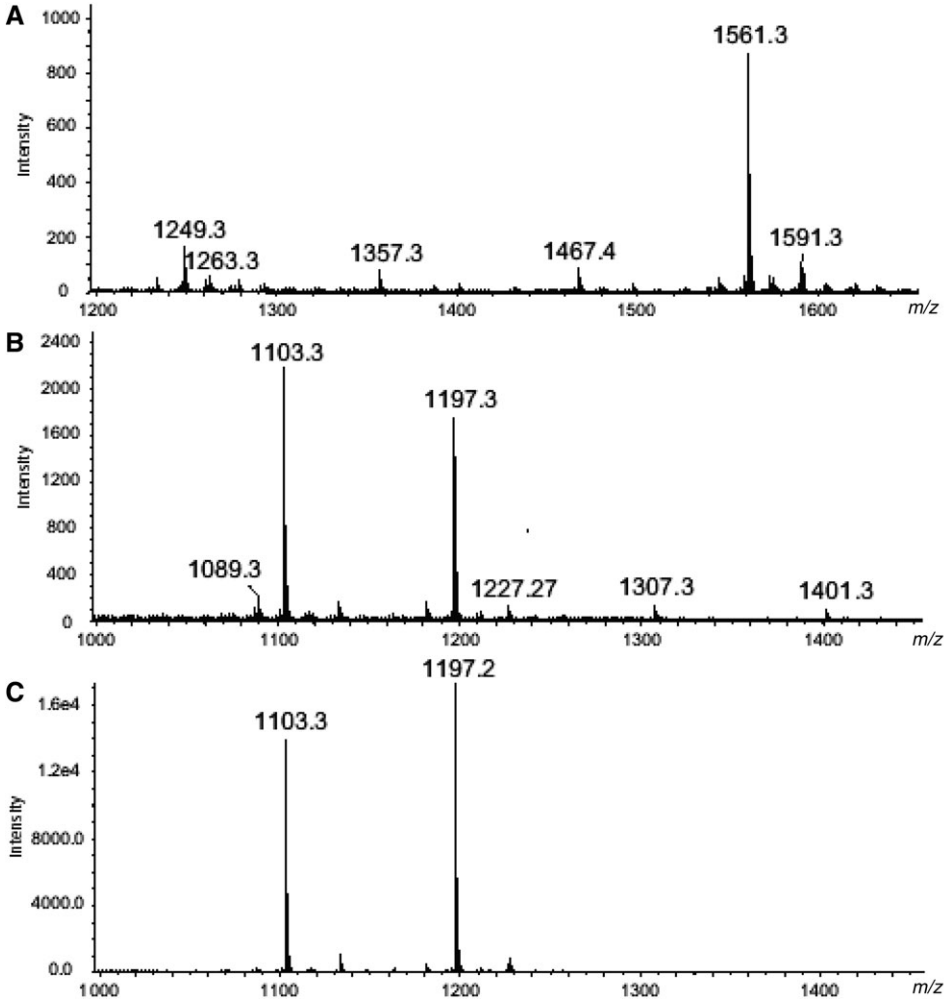

Fig. 3. ESI-MS analysis of permethylated PI-oligosaccharides released by alkaline hydrolysis from purified GIPCs of (**A**) KN99α wild-type strain; (**B**) NE321 mutant strain; and (**C**) NE178 mutant strain.

and C/Y secondary fragments ions following the release of phosphoryl group. These are completed by a full series of C-type fragment ions at m/z 259 (C_1), 463 (C_2), 667 (C_3), and 871 (C_4) separated by m/z 204, consistent with a linear arrangement of Hex residues. Then, fragmentation analysis on both permethylated derivatives of ion at m/z 1401 and native sample at m/z 1093 confirmed the presence of the linear PI-oligosaccharide Hex_5InsP in NE321 mutant strain (data not shown). As already mentioned, this isomer was not present in NE178 *Cryptococcus* mutant GIPCs.

NMR spectroscopy of PI-oligosaccharides

Subsequently, the structures inferred from ESI-MS were completed by NMR spectroscopy. PI-oligosaccharides released from GIPC of two mutant strains, NE178 and NE321, and of a wild-type strain KN99 of *C. neoformans* by alkaline hydrolysis were analyzed by proton NMR spectra, which were assigned from total correlation spectroscopy (TOCSY) experiments and the ^{13}C heteronuclear single quantum-correlation (HSQC) spectroscopy. Information on the linkage and sequence of the monosaccharides was obtained from rotating frame nuclear Overhauser enhancement spectroscopy (ROESY).

Five resonances were observed in the anomeric region of the 1D proton NMR spectrum of PI-oligosaccharide from NE178 mutant GIPC (Figure 6A) at 5.172, 5.129, 5.086, 4.820, and 4.468 ppm. Four of them at lower field were assigned as α-Man*p*, and the other one as β-Gal*p* residue. The α-anomeric configuration of Man units was established from the chemical shifts of H-3 and H-5 protons and the β-anomeric configuration of Gal from the magnitude $^3J_{H1\text{-}H2}$ from the chemical shifts of the H-1 and C-1. Almost all α-Man*p*, β-Gal*p*, and Ins resonances were unambiguously assigned from TOCSY and ^{13}C-HSQC experiments (Table I). As suggested by MS analyses, NMR data clearly established the presence of two compounds differing by the presence of either Ins or Ins-P in reducing position. The Ins residues from Ins-1-P designated Ins(1) and Ins designated Ins(1a) (Table I) were identified from the lack of their anomeric resonances and from the presence of two low-field signals at 4.257 and 4.094 ppm, respectively, which displayed nuclear Overhauser effects (NOEs) with Man(1) H-1 at 5.172 and Man(1a) at 5.086 ppm, in the ROESY spectrum (not shown). This Ins heterogeneity is due to the partial de-phosphorylation of Ins-1-P during the base-catalyzed hydrolysis of GIPCs. The resonances at 4.257 and 4.094 ppm were assumed to be H-2 of Ins(1) and Ins(1a),

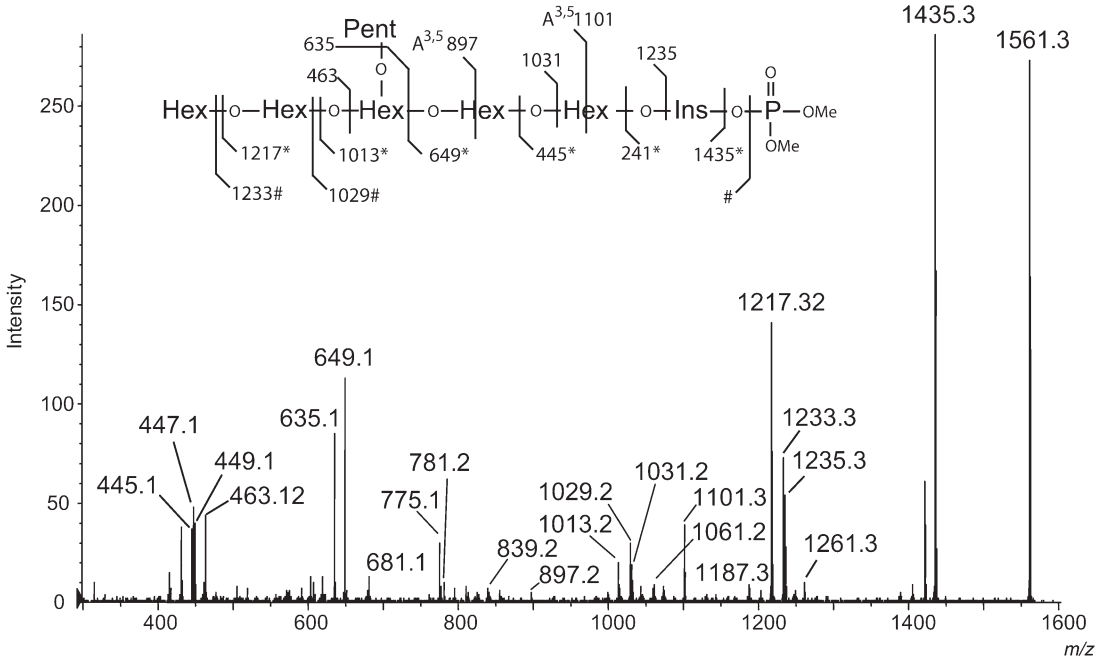

Fig. 4. ESI-MS/MS analysis of major permethylated PI-oligosaccharide from KN99α wild-type strain. Parent ion at m/z 1561 corresponding to permethylated Pent1Hex5InsP was fragmented. Asterisk indicates Y primary and B/Y secondary fragments and hash indicates Z primary and B/Z secondary fragments.

respectively, since the linkage between α-Man and Ins is (1→2) in all GIPC structures of *C. neoformans* so far determined (Heise et al. 2002). Furthermore, the spin system of Ins-1-P is in agreement with the published parameters of C2 substituted Ins-1-P from phosphatidyl-*myo*-Ins anchors of mycobacterial lipoglycans (Guerardel et al. 2002).

The monosaccharide sequence and the linkage found in the structure of PI-oligosaccharides were determined by ROESY spectrum. Inter-residue NOEs were observed between H-1 of β-Gal*p* and H-6 of α-Man*p*(1) at 3.871 ppm; between H-6 of α-Man*p*(1a) at 3.840 ppm and H-1 of α-Man*p*(2) at 4.820 ppm and H-4 of β-Gal*p* at 4.023 ppm; and between H-1 of α-Man*p*(3) at 5.129 ppm and H-3 of Man*p*(2) at 3.957 ppm (Table I). Further confirmation of these sequences was provided by ^{13}C chemical shift data (Table I). The C-3 resonance in the residue designated α-Man(2) was observed at low field at 81.04 ppm, whereas this value is typically 71–73 ppm for α-Man*p* (3), α-Man*p*(1), and for model systems in which the position 3 is not glycosylated. The low-field chemical shift of C-6 of α-Man*p*(1) at 71.34 ppm is consistent with glycosylation in the O-6 position. In disaccharide α-Man*p*-(1→6)-Man*p*, the C-6 signal is at 67 ppm (Jansson et al. 1994). On the basis of the NMR data, the PI-oligosaccharide structure of the NE178 mutant could be α-Man*p*(1→3)α-Man*p*(1→4)β-Gal*p*(β1→6)α-Man*p*(1→2)InsP.

The 1D proton NMR spectrum of the N321 mutant PI-oligosaccharide (Figure 6B) differed from that of NE178 (Figure 6A) by the presence of two minor anomeric proton resonances, which suggest a low degree of heterogeneity associated with the oligosaccharide chains. These signals were assigned to α-Man*p* residues designated Man(3a) at 5.16 ppm and Man(2a) at 4.99 ppm (Table II). In the ROESY spectrum NOEs were observed between H-1 of Man(3a) and H-2 of Man(2a) at 4.14 ppm (data not shown); and between H-1 Man(2a) and H-4 of Gal*p* at 4.023 ppm, which is consistent with a α(Man*p*(1→2)αMan*p*(1→4)βGal*p* sequence. The confirmation of this sequence was also provided by carbon chemical shift data obtained from HSQC spectrum (Table II) that showed the resonance at 77.88 ppm, assigned as C-2 of Man(2a) is shifted downfield compared with the corresponding C-2 of Man(2) signal in the PI-oligosaccharide NE178 (Table I). The remaining portion of the structure displayed an identical pattern of NOEs to the PI-oligosaccharide NE178. These data show that the PI-oligosacharidesfrom NE321 mutant is a mixture of two isomers: αMan*p*(1→3)αMan*p*(1→4)β-Gal*p*(β1→6)α-Man*p*(1→2) InsP, and αMan*p*(1→2)αMan*p*(1→4)βGal*p*(β1→6)αMan*p*(1-2)InsP.

The 1D proton NMR spectrum of PI-oligosaccharide from *C. neoformans* wild-type strain (Figure 6C) showed some similarities with the PI-oligosaccharide spectrum of NE178 (Figure 6A), except for the presence of three additional anomeric resonances. These were assigned to two α-Man*p* residues (5.122 and 4.89 ppm) and for β-Xyl*p* (4.354 ppm). The presence of α-Man*p* spin system at 5.122 ppm, designated Man*p*(1a), was attributed to the →6)αMan*p*(1→2)-Ins-6-P, resulting from phosphate migration during the GIPC alkaline hydrolysis. This additional Ins spin system designated Ins(1a′) was identified from the lack of its anomeric resonance and from the presence of a low-field H-2 at 4.087 ppm (Table III). In ROESY spectrum, an intense cross peak was observed between the H-2 of Ins at 4.087 ppm and H-1 of Man(1a′) at 5.122 ppm, indicating a 1→2 glycosidic linkage between these two residues. The Ins(1a′) spin system was supported by the presence of signals at low field of H-5 at 3.408 ppm, and of C-6 at 80 ppm (Table III).

In the wild-type PI-oligosaccharide, the sequence of and linkage between the sugar residues were deduced from the

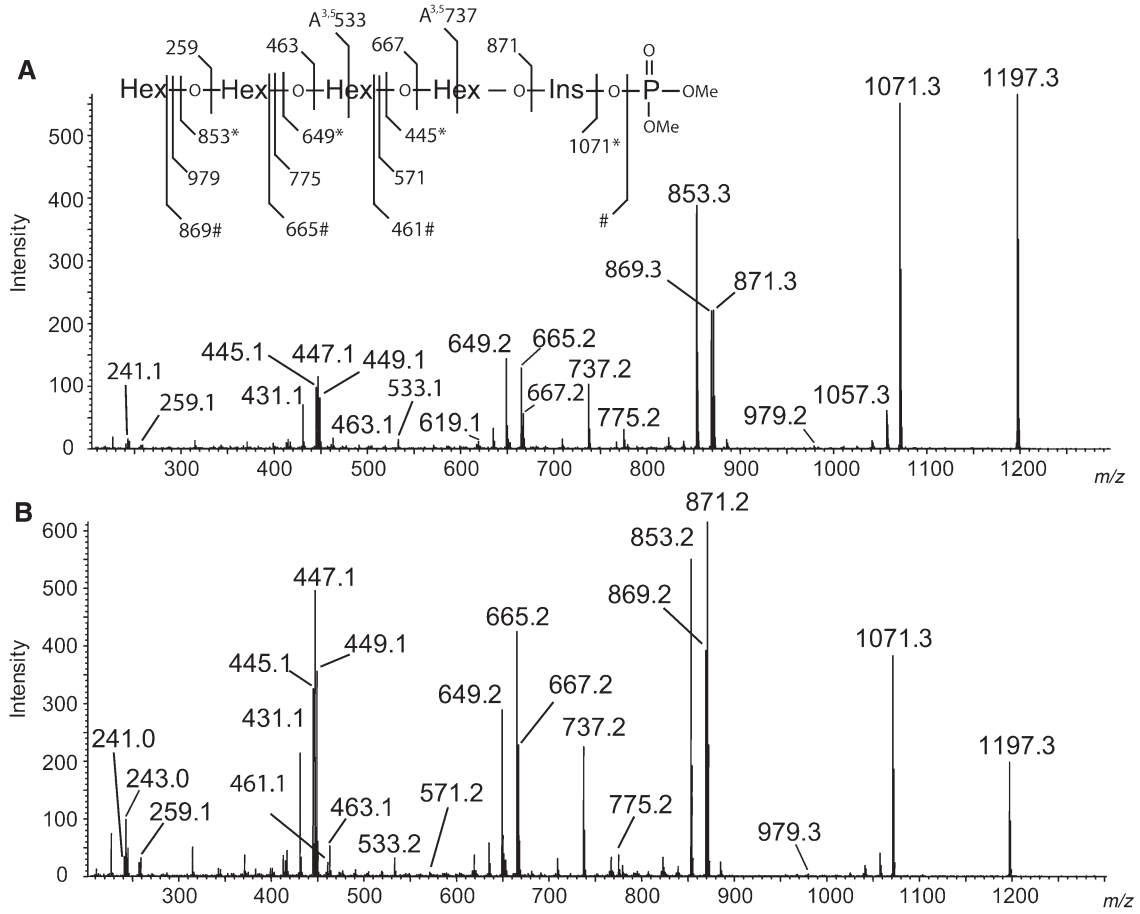

Fig. 5. ESI-MS/MS analysis of permethylated PI-oligosaccharides from NE321 mutant strain and NE178 mutant strains. Parent ions at m/z 1197 corresponding to permethylated Hex4InsP from (A) NE321 mutant strain and (B) NE178 mutant strain were fragmented.

following arguments: (i) the proton and carbon chemical shifts (Table III) are very similar to those of αMan*p*(1→6)αMan*p*(1→3)[βXyl*p*(1→2)]αMan*p*(1→4)βGal*p*(1→6)αMan*p*(1→2)InsP system found in the *C. neoformans* Ins-oligosaccharides obtained from GIPC of Cap67 mutant strain (Heise et al. 2002). As the Cap67 Ins-oligosaccharide was isolated from GIPC by amonolysis, the H-1 signals corresponding to Man linked to Ins(1) or Ins(1a′) was not observed and replaced by H-1 resonance of Man (1a); (ii) the ESI-MS/MS analysis showed unambigously that the Xyl is terminally located on the Man(2) (Table III); (iii) in ROESY spectrum (not shown), an NOE between H-1 of Man(4) and H-5 and H-6 of Man(3) at 3.889 and 3.651 ppm, respectively, suggested a 1→6 linkage between them. The high-field position 102.39 ppm of the C-1 resonance of Man(4) is consistent with an αMan*p*(1→6)-linked residue. The H-1 resonance of Man(3) in turn displayed an inter-residue NOE with H-3 of Man(2) at 4.010 ppm, providing evidence of an α(1→3) linkage. The anomeric proton of the terminal Xyl residue showed NOEs between H-1 and H-2 of Man(2) at 4.972 and 4.047, respectively. This result is consistent with a βXyl(1→2)Man branch, which was confirmed by the low-field position of the C-2 chemical shift of the Man(2) at 80.83 ppm. The remaining NOEs between Man(2), Gal, Man(1), and Ins were as was described for the PI-oligosaccharide from NE178 mutant strain; and (iv) the additional confirmation of the wild-type PI-oligosaccharide sequence was provided by carbon chemical shifts data (Table III). The structures of the PI-oligosaccharides from *C. neoformans* KN99α wild-type, NE321, and NE178 mutant strains are summarized in Table IV.

Discussion

In this study, we present evidence that the monoxylosyl side chain is necessary for the GIPC synthesis in which Man is added to αMan*p*(1→3)[β-Xyl*p*1→2] αMan*p*(1→4)Gal*p*(β1→6)α-Man*p*(1→2)InsPC to form the major and terminal GIPC of *C. neoformans* wild-type strain: αMan*p*(1→6)αMan*p*(1→3)[β-Xyl*p*1→2] αMan*p*(1→4)Gal*p*(β1→6)α-Man*p*(1→2)InsPC. This conclusion is supported by comparative data from MS and NMR spectroscopy analyses of GIPCs isolated from KN99α strain (Nielsen et al. 2003) with those from mutant strains that lack UDP-Xyl, by disruption of either UDP-Glc dehydrogenase (*ugd1*Δ) (NE341) (Moyrand and Janbon 2004) or UDP-glucuronic acid (GlcA) descarboxylase (*uxs1*Δ) (NE178) (Moyrand et al. 2002) genes.

The predominant and largest GIPC that accumulated in the wild-type was found to be αMan*p*(1→6)αMan*p*(1→3)[β-Xyl*p*1→2]αMan*p*(1→4)Gal*p*(β1→6)α-Man*p*(1→2) InsPC, whereas in both mutants the most abundant species was

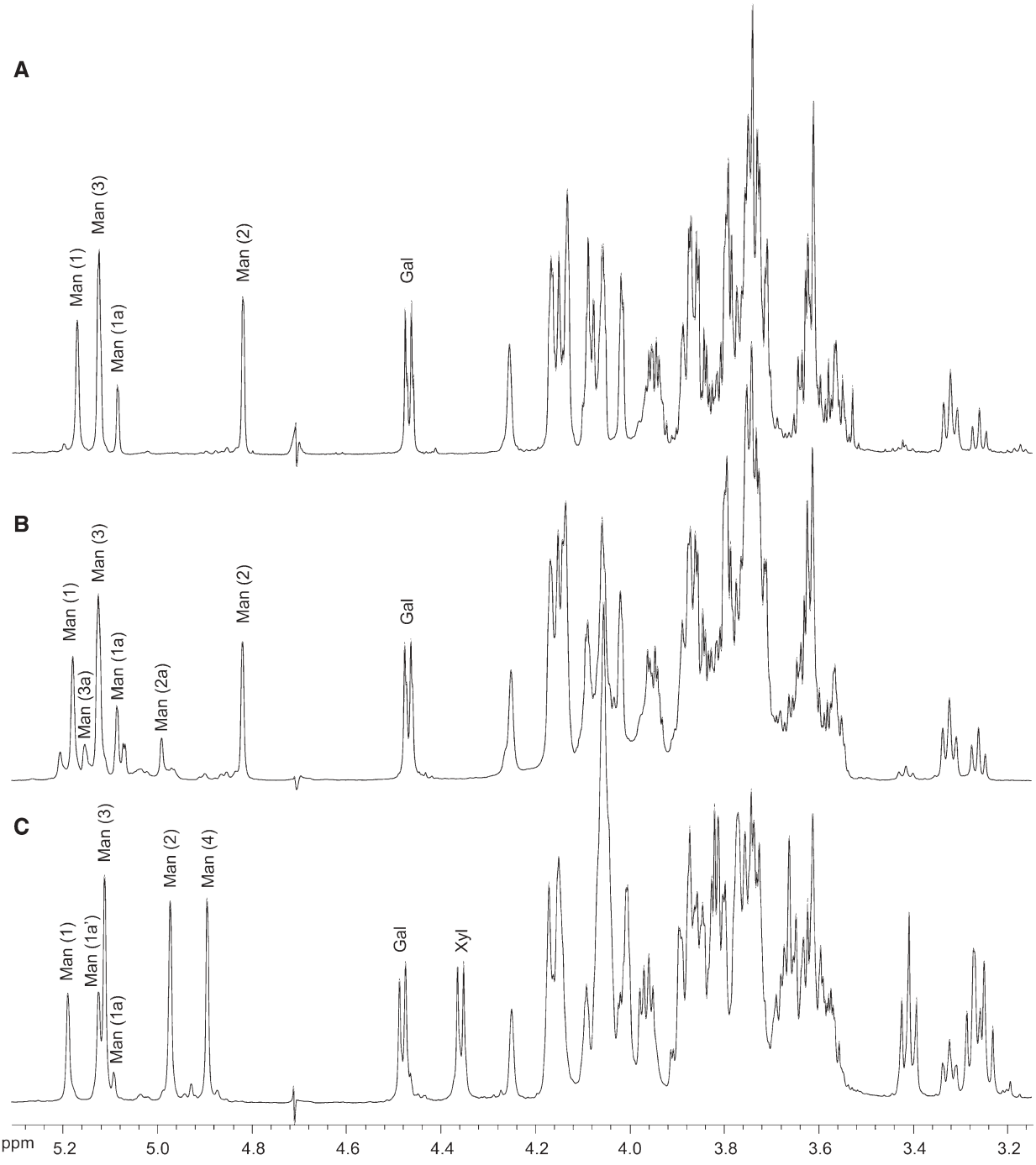

Fig. 6. Partial 600 MHz ^{1}H NMR spectra of PI-oligosaccharides of GIPCs from *C. neoformans* strains. (**A**) NE178; (**B**); NE321; and (**C**) KN99α.

identified as αMan*p*(1→3)αMan*p*(1→4)Gal*p*(β1→6)α-Man*p*(1→2)InsPC.

The observation that the absence of side chain donor, UDP-Xyl, impairs the glycan backbone to be extended beyond α(1→3) linked Man strongly suggests that the addition of Xyl is required for *C. neoformans* to synthesize more elaborated GIPCs. The lack of terminal α(1→6)Man*p* in both mutant strains must be due to the inability of a putative α(1→6)-mannosyltransferase to utilize αMan*p*(1→3)αMan*p*(1→4)Gal*p*(β1→6)α-Man*p*(1→2)InsPC as acceptor substrate. However, we have previously reported that αMan*p*(1→3)[β-Xyl*p*1→2] αMan*p*(1→4)Gal*p*(β1→6)α-Man*p*(1→2)InsPC was the main and largest GIPC formed in *C. neoformans* wild-type 444 strain (Heise *et al.* 2002). As

Table I. ^{1}H and ^{13}C assignments (ppm) of the PI-oligosaccharide of *C. neoformans* NE178 mutant

	α-Man*p* (1→3)	α-Man*p* (1→4)	β-Gal*p* (1→6)	α-Man*p* (1→2)		Ins-1-OPO_3 or Ins	
	(3)	(2)		(1)	(1a)	(1)	(1a)
H-1	5.129	4.820	4.468	5.172	5.086	3.963	3.797
H-2	4.051	4.173	3.566	4.130	4.086	4.257	4.094
H-3	3.856	3.957	3.716	3.856	3.846	3.611	3.556
H-4	3.742	3.793	4.023	3.742	3.770	3.744	3.623
H-5	4.071	4.069	3.736	4.150	4.099	3.325	3.254
H-6	3.734	3.807	3.735	4.142	4.153	3.874	3.816
H-6′	3.876	3.795	3.735	3.871	3.840		
C-1	104.97	104.33	106.13	104.32	104.33	77.81	73.02
C-2	72.76	72.37	73.66	72.76	72.76	82.16	83.13
C-3	73.01	81.04	74.70	73.02	72.91	76.09	75.27
C-4	69.26	68.49	80.26	69.26	69.65	73.02	72.93
C-5	75.86	75.86	75.10	74.44	73.65	77.22	77.53
C-6	63.83	63.18	63.18	71.34	69.14	73.07	73.12

the αMan*p*(1→3)[β-Xyl*p*1→2]αMan*p*(1→4)Gal*p*(β1→6)α-Man*p*(1→2)InsPC must be the precursor of αMan*p*(1→6)α-Man*p*(1→3)[β-Xyl*p*1→2]αMan*p*(1→4)Gal*p*(β1→6)α-Man*p*(1→2)InsPC, the absence α(1→6) linked Man GIPC of *C. neoformans* 444 strain (Heise *et al.* 2002) could be due to either the lack of the gene encoding an α(1→6)-mannosyltransferase or this transferase is inactive to elongate the αMan*p*(1→3)[β-Xyl*p*1→2]αMan*p*(1→4)Gal*p*β1→6)α-Man*p*(1→2)InsPC. We do not know yet whether the structural difference among GIPCs from different *C. neoformans* strains are a common feature of this species or whether it is somehow related to the virulence.

Surprisingly, only *C. neoformans* cells lacking UDP-Glc dehydrogenase, and consequently unable to produce UDP-GlcA and UDP-Xyl, were able to synthesize minor GIPCs components. One such a GIPC was identified as an αMan*p*(1→2)αMan*p*(1→4)Gal*p*(β1→6)α-Man*p*(1→2) InsPC (Table IV). The presence of GIPC isomer as minor component, only in the *ugd1*Δ mutant strain is not well understood, as identical precursor could also be found in the encapsulated *uxs1*Δ mutant strain. Presumably, minor GIPC species could have been synthesized as a compensatory effect to replace the absent polysaccharide capsule in the *ugd1*Δ mutant. Pleiotropic effects to compensate mutations that affect phospholipomannan, and capsule polysaccharide biosynthesis have been described in *C. albicans* (Mille et al. 2004), and *C. neoformans* (Heise et al. 2002), respectively.

Interestingly, our results show that GIPC and capsular GalXM (Vaishnav et al. 1998) from *C. neoformans* share some structural features. Indeed, the outer portion of the GIPC glycan chain differs from the GalXM side chain (Vaishnav et al. 1998) in that the β(1→2)Xyl is always present, whereas β(1→3)Xyl residue is not. As a number of confirmed or putative genes for β(1→2)-xylosyltransferase (Klutts et al. 2006) and α(1→3)-mannosyltransferase (Sommer et al. 2003) are known, an important question to be answered is whether some glycosylation steps in the GIPC biosynthetic pathway are catalyzed by glycosyltransferases also used in GalXM biosynthesis. Another important point that remains to be determined in GIPC biosynthesis is whether the addition of Xyl unit occurs before or after the precursor αMan*p*(1→4)Gal*p*(β1→6)α-Man*p*(1→2)InsPC is substituted by an α(1→3)-linked Man.

Material and methods

Strains and growth conditions

The *uxs1*Δ mutant strain NE178 (deleted in the fungal gene encoding UDP-GlcA descarboxylase) (Moyrand et al. 2002), the *ugd1*Δ mutant strain NE321 (deleted in the fungal gene encoding UDP-Glc dehydrogenase) (Moyrand and Janbon 2004), and the wild-type strain KN99α (Nielsen et al. 2003)

Table II. ^{1}H and ^{13}C assignments (ppm) of the PI-oligosaccharide of *C. neoformans* NE321 mutant

	α-Man*p* (1→3)		α-Man*p* (1→4)		β-Gal*p* (1→6)	α-Man*p* (1→2)		Ins-1-OPO_3 or Ins	
	(3)	(3a)	(2)	(2a)		(1)	(1a)	(1)	(1a)
H-1	5.127	5.164	4.818	4.993	4.465	5.171	5.084	3.962	3.797
H-2	4.052	4.058	4.172	4.140	3.564	4.131	4.086	4.257	4.092
H-3	3.855	—	3.956	—	3.714	3.855	3.846	3.610	3.554
H-4	3.742	—	3.792	—	4.024	3.740	3.774	3.743	3.623
H-5	4.070	—	4.068	—	3.735	4.151	4.010	3.324	3.254
H-6	3.732	—	3.806	—	3.733	4.140	4.151	3.874	3.816
H-6′	3.874	—	3.793	—	3.734	3.872	3.842	—	—
C-1	104.97	104.35	104.33	101.25	106.13	104.32	104.33	77.80	73.02
C-2	72.76	72.75	72.37	77.81	73.66	72.76	72.76	82.16	83.13
C-3	73.01		81.04		74.70	73.02	72.91	76.08	75.27
C-4	69.26		68.49		80.26	69.26	69.65	73.01	72.93
C-5	75.86		75.86		75.10	74.44	73.65	77.23	77.55
C-6	63.83		63.18		63.18	71.34	69.14	73.04	73.12

Table III. ^{1}H and ^{13}C assignments (ppm) of the PI-oligosaccharide of *C. neoformans* KN99α wild-type

	α-Man*p* (1→6)	α-Man*p* (1→3)	[β-Xyl*p* (1→2)]	α-Man*p* (1→4)	β-Gal*p* (1→6)	α-Man*p* (1→2)			Ins-1/6-OPO_3 or Ins		
	(4)	(3)		(2)		(1)	(1a′)	(1a)	(1)	(1a′)	(1a)
H1	4.893	5.103	4.354	4.972	4.479	5.188	5.122	5.083	3.974	3.684	3.663
H2	4.004	4.056	3.268	4.047	3.574	4.147	4.169	4.085	4.248	4.087	4.092
H3	3.852	3.819	3.405	4.010	3.732	3.846	3.896	3.845	3.612	3.610	3.554
H4	3.665	3.820	3.609	3.867	4.067	3.740	3.744	3.772	3.731	3.662	3.254
H5	3.650	3.889	3.963	4.058	3.738	4.154	4.169	4.009	3.320	3.408	3.621
H6/ H5′	3.876	3.859	3.248	3.833	3.725	4.154	4.155	4.152	3.856	4.009	3.816
H6′	3.742	3.651		3.804	3.760	3.875	3.876	3.842			
C1	102.39	105.77	105.77	101.93	106.23	104.24	104.35	104.33	77.81	74.53	73.02
C2	72.63	72.79	75.41	80.76	73.57	72.79	72.82	72.76	82.29	82.46	83.07
C3	73.36	73.42	78.21	80.00	74.78	72.95	72.96	72.91	76.05	75.26	75.21
C4	69.45	68.68	72.93	68.80	79.84	69.31	69.31	69.65	73.08	72.97	72.90
C5	75.35	72.96	67.87	74.17	75.20	74.49	74.51	73.65	77.20	77.10	77.56
C6	63.69	68.79		62.81	63.20	71.47	71.48	69.14	73.02	80.00	73.12

were kindly provided by Dr Guilhem Janbon (Institut Pasteur, Paris, France). Cells were cultured on yeast extract-peptone-dextrose (YPD) medium (Sherman 1992) at 30 °C in a shaker at 100 rpm. After 5 days, the cells were collected by centrifugation (7000*g*, 15 min, 4 °C) and washed three times with 0.9% NaCl.

Extraction and purification of glycoinositolphosphoryl ceramides

The *Cryptococcus* cells were extracted with aqueous phenol, and GIPCs present in the aqueous layer were solubilized in chloroform/methanol/water (10:10:3, v/v/v) as previously described (Penha et al. 2001). For purification, GIPCs were dissolved in 5% propan-1-ol in 0.1 M ammonium acetate (Solvent A) and applied to a column of octyl-Sepharose (20 cm × 1 cm) at a flow rate of 10 mL h^{-1}. After washing with 20 mL Solvent A and 20 mL of 5% propan-1-ol, the column was eluted using a propan-1-ol linear gradient (5–65%) at a flow rate of 16 mL h^{-1}. Sixty-two milliliter fractions were collected and screened for homogeneity by HPTLC (silica gel 60 plates, Merck) using chloform/methanol/1M NH_4OH (10:10:3, v/v/v) as mobile phase. GIPCs were detected by spraying the plates with orcinol/sulfuric acid (Humbel and Collaert 1975).

Carbohydrate and inositol analyses

The monosaccharide composition of GIPCs was determined according to Sweeley et al. (1963). After methanolysis with 0.5 M HCl in methanol (18 h, 80 °C), the mixture was extracted with hexane and the methanolic phase neutralized with Ag_2CO_3. The products were *N*-acetylated with acetic anhydride, dried, and treated with bis-(trimethylsilyl)trifluoroacetamide (BSTFA)/pyridine (1:1, v/v, 1 h, room temperature). Trimethylsilyl derivatives were analyzed by gas-chromatography (GC) using a DB-5 fused silica capillary column (25 m × 0.25 mm i.d.) with hydrogen (10 psi) as the carrier gas. The column temperature was programmed from 120 °C to 240 °C at 2 °C/min. For the analysis of Ins, GIPCs were hydrolyzed with 6 M HCl (18 h at 105 °C), dried, treated with BSTFA/pyridine (1:1, v/v, 1 h, room temperature), and analyzed by GC using a DB-5 fused silica capillary column (25 m × 0.25 mm i.d.) with hydrogen (10 psi) as the carrier gas. Peaks were identified by comparison of their retention times to authentic standards and by GC-MS.

Lipid analysis

After methanolysis of the GIPC with methanolic-HCl (18 h at 80 °C), fatty acid methyl esters (FAMES) were extracted with

Table IV. Structures of PI-oligosaccharides of GIPCs isolated from *C. neoformans* strains

C. neoformans strain— PI-oligosaccharides	Structure
KN99α	β-Xyl*p* 1 ↓ 2 α-Man*p*-(1→6)-α-Man*p*-(1→3)-α-Man*p*-(1→4)-β-Gal*p*-(1→6)-α-Man*p*-(1→2)-Ins-1P
NE321	α-Man*p*-(1→3)-α-Man*p*-(1→4)-β-Gal*p*-(1→6)-α-Man*p*-(1→2)-Ins-1P α-Man*p*-(1→2)-α-Man*p*-(1→4)-β-Gal*p*-(1→6)-α-Man*p*-(1→2)-Ins-1P
NE178	α-Man*p*-(1→3)-α-Man*p*-(1→4)-β-Gal*p*-(1→6)-α-Man*p*-(1→2)-Ins-1P

hexane. The extracts were concentrated and analyzed by GC after derivatization with BSTFA/pyridine as described in *Carbohydrate and inositol analyses*. The column temperature was programmed from 180 °C to 280 °C at 3 °C/min. Peaks were identified by their retention time compared with authentic standards and by GC-MS. For the analysis of long-chain bases, GIPCs were methanolyzed (1 M methanol-HCl made 10 M with respect to water) (Carter and Gaver 1967) for 18 h at 80 °C. After adjusting the pH to about 11 with aqueous NaOH, long-chain bases were extracted with diethyl ether. The extracts were washed with water, dried with anhydrous sodium sulfate, evaporated to dryness, dissolved in methanol, and *N*-acetylated with acetic anhydride (18 h, room temperature in the dark). The product was treated with BSTFA/pyridine and analyzed by GC and GC-MS as described for the FAMEs.

Isolation, purification, and permethylation of phosphoinositol (PI) oligosaccharides

GIPCs were submitted to alkaline hydrolysis (1 M KOH, 2 h, 100 °C). After neutralization with acetic acid, the material was passed through a column (2 cm × 4 cm) of Dowex 50-X8 (25–50 mesh, H^+form). The PI-oligosaccharides were eluted with water and fractionated on a Bio Gel P-4 (extra fine) column (1 cm × 30 cm). Fractions of 1 mL were collected and assayed for carbohydrate by spoting 5 μL onto a thin layer chromatography plate which was sprayed with orcinol/sulfuric acid (Humbel and Collaert 1975). Carbohydrate-containing fractions were pooled and lyophilized. The PI-oligosaccharides were permethylated by the procedure of Ciucanu and Kerek (1984).

Matrix-assisted laser desorption/ionization time-of-flight mass spectrometer

MALDI mass spectra were recorded with a Voyager DE-PRO MALDI-TOF spectrometer (Applied Biosystems/MDS Sciex, Toronto, Canada), equipped with a 337 nm nitrogen laser. The instrument was operated in the negative ion reflectron mode at 20 kV accelerating voltage with time-lag focussing enabled. Samples were dissolved in 5% formic acid, and 1 μL was mixed with an equal volume of norharmane matrix solution (10 mg/mL in 50% acetonitrile) and air dried on the stainless steel target. Spectra were externally calibrated using deprotonated molecules of angiotensin I (m/z 1294.670) and ACTH clip18-34 (m/z 2463.183) as references.

For nano-ESI-MS, analyses were performed using a Q-STAR Pulsar quadrupole time-flight (Q-TOF) mass spectrometer (Applied Biosystems) fitted with a nanoelectrospray ion source (Protana, Odense, Denmark). Glycans dissolved in a solution of 50% methanol and 1% formic acid (0.5 pmol/μL) were sprayed from gold-coated "medium length" borosilicate capillaries (Protana). A potential of 800 V was applied to the capillary tip. For generation of MS/MS data, the precursor ion was selected by the quadrupole, and was subsequently fragmented in the collision cell using nitrogen at a pressure of about 5.3×10^{-5} Torr and appropriate collision energy. The CID spectra were recorded by the orthogonal TOF analyzer over the range m/z 50–2000.

Nuclear magnetic resonance spectroscopy

NMR spectra were obtained on a Bruker Unity 600 spectrometer equipped with pulsed field gradients (PFG) and a 5 mm PFG triple resonance probe, at a probe temperature of 30 °C. Standard pulse sequences were used for 1D proton, TOCSY and ROESY spectra, except for the inclusion of spin-echo sequences into the TOCSY and ROESY pulse programs. Mixing times were 80 ms in the TOCSY and 150 ms in the ROESY spectra. Heteronuclear correlation spectra were obtained using the sequence of Wider and Wuthrich (1993) employing pulsed field gradients to suppress unwanted signals. These were optimized for $^1J_{C,H}$ of 150 Hz (delay = 3.3 ms) or for $^nJ_{C,H}$ of 20 Hz (delay = 25 ms). Proton and ^{13}C chemical shifts were referenced to internal acetone at 2.225 and 31.50 ppm, respectively.

Acknowledgments

The authors gratefully acknowledge the excellent technical support of Orlando Augusto Agrellos Filho. The *uxs1*Δ mutant NE178; *ugd1*Δ mutant NE321; and wild-type KN99α *Cryptococcus* strains were kindly provided by Dr Guilhem Janbon from Institut Pasteur, Paris, France. This work was supported by Conselho Nacional de Desenvolvimento Científico e Tecnológico (CNPq); Fundação de Amparo à Pesquisa do Estado do Rio de Janeiro (FAPERJ) and The Millenium Institute/CNPq.

Conflict of interest statement

None declared.

Abbreviations

AIDS, acquired immune deficiency syndrome; BSTFA, bis-(trimethylsilyl)trifluoroacetamide; ESI, electrospray ionization; ESI-MS, electrospray ionization mass spectrometry; GC, gas chromatography; GIPC, glycoinositolphosphoryl ceramide; GlcA, glucuronic acid; Gal, galactose; GalXM, galactoxylomannan; GXM, glucuronoxylomannan; Hex, hexose; HPTLC, high-performance thin layer chromatography; HSQC, heteronuclear single-quantum correlation; Ins, inositol; MALDI-TOF, matrix-assisted laser desorption/ionization time-of-flight; Man, mannose; MIPC, mannose inositol phosphoryl ceramide; MS, mass spectrometry; NMR, nuclear magnetic resonance; NOE, nuclear Overhauser effect; Pen, pentose; PI, phosphatidylinositol; ROESY, rotating frame nuclear Overhauser enhancement spectroscopy; TOCSY, total correlation spectroscopy; Xyl, xylose.

References

Barr K, Lester RL. 1984. Occurrence of novel antigenic phosphoinositol-containing sphingolipids in the pathogenic yeast *Histoplasma capsulatum*. Biochemistry. 23:5581–5588.

Barr K, Laine RA, Lester RL. 1984. Carbohydrate structures of three novel phosphoinositol-containing sphingolipids from the yeast *Histoplasma capsulatum*. Biochemistry. 23:5589–5596.

Bennion B, Park C, Fuller M, Lindsey R, Momany M, Jennemann R, Levery SB. 2003. Glycosphingolipids of the model fungus *Aspergillus nidulans*: characterization of GIPCs with oligo-α-mannose-type glycans. J Lip Res. 44:2073–2088.

Carter HE, Gaver RC. 1967. Branched-chain sphingosines from *Tetrahymena pyriformes*. Biochem Biophys Res Commun. 29:886–891.

Ciucanu I, Kerek F. 1984. A simple and rapid method for the permethylation of carbohydrates. Carbohydr Res. 131:403–409.

Dickson RC, Lester RL. 2002. Sphingolipid functions in *Saccharomyces cerevisiae*. Biochim Biophys Acta. 1583:13–25.

Guerardel Y, Maes E, Elass E, Leroy Y, Timmerman P, Besra GS, Locht C, Strecker G, Kremer L. 2002. Structural study of lipomannan and lipoarabinomannan from *Mycobacterium chelonae*. Presence of unusual components with alpha 1,3-mannopyranose side chains. J Biol Chem. 277: 30635–30648.

Heise N, Gutierrez ALS, Mattos KA, Jones C, Wait R, Previato JO, Mendonça-Previato L. 2002. Molecular analysis of a novel family of complex glycoinositolphosphoryl ceramides from *Cryptococcus neoformans*: structural differences between encapsulated and acapsular yeast forms. Glycobiology. 12:409–420.

Humbel R, Collaert M. 1975. Oligosaccharides in urine of patients with glycoprotein storage diseases. I. Rapid detection by thin-layer chromatography. Clin Chim Acta. 60:143–145.

Jansson P-E, Kenne L, Kolare I. 1994. NMR studies of some (1→6)-linked disaccharide methyl glycosides. Carbohydr Res. 257:163–174.

Klutts JS, Yoneda A, Reilly MC, Bose I, Doering T. 2006. Glycosyltransferase and their products: cryptococcal variations on fungal themes. FEMS Yeast Res. 6:499–512.

Levery SB, Toledo MS, Straus AH, Takahashi HK. 1998. Structure elucidation of sphingolipids from the mycopathogen *P. brasiliensis*: an immunodominant β-galactofuranose residue is carried by a novel glycosylinositol phosphorylceramide antigen. Biochemistry. 37:8764–8775.

Mandala SM, Thornton RA, Milligan J, Rosenbach M, Garcia-Calvo M, Bull HG, Harris GH, Abruzzo K, Flaterry AM, Gill GJ, et al. 1998. Rustimicin, a potent antifungal agent, inhibits sphingolipid synthesis at inositol phosphoceramide synthase. J Biol Chem. 273:4942–14949.

Mandala SM, Thornton RA, Rosenbach M, Milligan J, Garcia-Calvo M, Bull HG, Kurtz MB. 1997. Khafrefungin, a novel inhibitor of sphingolipid synthesis. J Biol Chem. 272:32709–32714.

Mille C, Janbon G, Delplace F, Ibata-Ombetta S, Gaillardin C, Strecker G, Jouault T, Trinel P-A, Poulain D. 2004. Inactivation of *CaMIT1* inhibits *Candida albicans* phospholipomannan β-mannosylation, reduces virulence, and alters cell wall protein β-mannosylation. J Biol Chem. 279: 47952–47960.

Mitchell TG, Perfect JR. 1995. Cryptococcosis in the era of AIDS – 100 years after the discovery of *Cryptococcus neoformans*. Clin Microbiol Rev. 8: 515–548, 1995.

Moyrand F, Janbon G. 2004. *UGD1*, encoding the *Cryptococcus neoformans* UDP-glucose dehydrogenase, is essential for growth at 37 °C and for capsule biosynthesis. Eukariot Cell. 3:1601–1608.

Moyrand F, Klaproth B, Himmelreich U, Dromer F, Janbon G. 2002. Isolation and characterization of capsule structure mutant strains of *Cryptococcus neoformans*. Mol Microbiol. 45:837–849.

Nagiec MM, Nagiec EE, Baltisberger JA, Wells GB, Lester RL, Dickson RC. 1997. Sphingolipid synthesis as a target for antifungal drugs. Complementation of the inositol phosphorylceramide synthase defect in a mutant strain of *Sacchoromyces cerevisae* by the *AUR1* gene. J Biol Chem. 272:9809–9817.

Nielsen K, Cox GM, Wang P, Toffaletti DL, Perfect JR, Heitman J. 2003. Sexual cycle of *Cryptococcus neoformans* var. *grubii* and virulence of congenic a and α isolates. Infec Immun. 71:4831–4841.

Penha CVL, Todeschini AR, Lopes-Bezerra LM, Wait R, Jones C, Mattos KA, Heise N, Mendonça-Previato Previato JO. 2001. Characterization of novel structures of mannosylphosphoryl ceramides from the yeast forms of *Sporothrix schenckii*. Eur J Biochem. 268:4243–4250.

Penha CVL, Lopes LM, Wait R, Jones C, Todeschici AR, Heise N, Mendonça-Previato L, Previato JO. 2000. A novel family of glycophosphosphingolipid expressed by yeast forms of *Sporothrix schenckii*: evidence for a unique Manα1→6Ins-phosphorylceramide substructure. Glycobiology. 10:1125.

Sherman F. 1992. Getting started with yeast. Methods Enzymol. 194:3–21.

Smith SW, Lester RL.1974. Inositol phosphorylceramide, a novel substance and chief member of a major group of yeast sphingolipids containing a single inositol phosphate. J Biol Chem. 249:3395–3405.

Sommer U, Liu H, Doering TL. 2003. An α-1,3-Mannosyltransferase of *Cryptococcus neoformans*. J Biol Chem. 278:47724–47730.

Sweeley CC, Bentley R, Makita M, Wells WW. 1963. Gas-liquid chromatography of trimethylsilyl derivatives of sugars and related substances. J Am Chem Soc. 85:2497.

Takesako K, Kuroda H, Inque T, Haruna F, Yoshikawa Y, Kato I. 1993. Biological properties of Aureobasidina A, a cyclic depsipeptide antifungal antibiotic. J Antibiot. 46:1414–1420.

Thevissen K, Cammue BP, Lemaire K, Winderickx J, Dickson RC, Lester RL, Ferket KK, Van ven F, Parret AH, Broekaert WF. 2000. A gene encoding a sphingolipid biosynthesis enzyme determines the sensitivity of *Saccharomyces cerevisiae* to an antifungal plant defensin from dahlia (*Dahlia merckii*). Proc Natl Acad Sci USA. 97:9531–9536.

Vaishnav V, Bacon BE, O'Neil M, Cherniak R. 1998. Structural characterization of the galactoxylomannan of *Cryptococcus neoformans* Cap67. Carbohydr Res. 306:315–330.

Wider G, Wuthrich K. 1993. A simple experimental scheme using pulsed-field gradients for coherence-pathway rejection and solvent suppression in phase-sensitive heteronuclear correlation spectra. J Magn Reson B. 102: 239–241.

Zink S, Mehlgarten C, Kitamoto HK, Nagase J, Jablonowski D, Dickson RC, Stark MJR, Schaffrath R. 2005. Mannosyl-diinositolphospho-ceramide, the major yeast plasm membrane sphingolipid, governs toxicity of *Kluyveromyces lactis* zymocin. Eukaryot Cell. 4:879–889.

Zhong W, Jeffries MW, Georgopapadakou NH. 2000. Inhibition of inositol phosphorylceramide synthase by aureobasidin A in *Candida* and *Aspergillus* species. Antimicrob Agents Chemother. 44:651–653.